Crystal structure of an integral membrane light-harvesting complex from photosynthetic bacteria

G. McDermott*, S. M. Prince*, A. A. Freer*, A. M. Hawthornthwaite-Lawless†, M. Z. Papiz†, R. J. Cogdell‡ & N. W. Isaacs*§

* Department of Chemistry and ‡ Division of Biochemistry and Molecular Biology, University of Glasgow, Glasgow G12 8QQ, UK
† DRAL Daresbury Laboratory, Daresbury, Warrington WA4 4AD, UK

The crystal structure of the light-harvesting antenna complex (LH2) from *Rhodopseudomonas acidophila* strain 10050 shows that the active assembly consists of two concentric cylinders of helical protein subunits which enclose the pigment molecules. Eighteen bacteriochlorophyll *a* molecules sandwiched between the helices form a continuous overlapping ring, and a further nine are positioned between the outer helices with the bacteriochlorin rings perpendicular to the transmembrane helix axis. There is an elegant intertwining of the bacteriochlorophyll phytol chains with carotenoid, which spans the complex.

THE initial event in bacterial photosynthesis is the absorption of a photon by the light-harvesting antenna system, which is followed by a rapid and efficient transfer of this energy to the reaction centre, where 'trapping' occurs[1]. Typically, purple bacteria contain two types of antenna complexes, both of which are integral membrane proteins[2]. The first type, LH1, is intimately associated with the reaction centre forming the so-called 'core' complex. Arranged more peripherally to this, and present in variable amounts, is the second type, LH2. Both types of complex are built on a similar modular principle[3]. The light-absorbing pigments, bacteriochlorophyll *a* (Bchl *a*) and carotenoids, are non-covalently bound to two low-molecular-weight hydrophobic apoproteins, α and β. The native complexes are oligomers of these components.

Here we present the crystal structure of the LH2 (B800–850) complex from the purple non-sulphur photosynthetic bacterium *Rhodopseudomonas acidophila* strain 10050. The complex contains bacteriochlorophyll (Bchl) *a* and rhodopin-glucoside pigments[4]. The α-apoprotein contains 53 amino acids, and the β-apoprotein 41. Both proteins have been sequenced[3].

The Bchl *a* molecules in this complex are divided into two spectral forms[2] which absorb at 800 nm and 850 nm. Circular dichroism analysis of these absorption bands has led to the conclusion that the Bchl *a* molecules that absorb at 800 nm are largely monomeric, whereas those absorbing at 850 nm are strongly exciton-coupled[5]. Conserved histidine residues in the apoproteins have been shown, by resonance Raman spectroscopy, to be liganded to the Mg at the centre of the Bchl *a* that absorbs at 850 nm[6]. The observation of efficient singlet–singlet energy transfer (>50%)[7] from the carotenoid to Bchl *a* has been interpreted to indicate that the π-electron system in the two pigment types must be within van der Waals contact[8].

Structure determination

Crystals of the LH2 complex from *Rps acidophila* strain 10050 were grown using a protocol based on that reported previously[9]. A marked improvement in the reproducibility and resolution of diffraction of the crystals was achieved using methods of separation based on size rather than charge. The integrity of the complex was monitored at each stage of the preparation by recording the absorption spectrum over the range 250–900 nm. The characteristic Bchl *a* spectrum is sensitive to the precise environment of the Bchl *a*. Spectra recorded from crystals are identical to those from whole cells (unpublished data), indicating that both contain the same complex assembly. The complex forms tabular crystals, space group *R*32, with hexagonal cell dimensions $a = b = 120.3$ Å, $c = 296.2$ Å. The structure has been determined to a resolution of 2.5 Å with diffraction data collected at a synchrotron source, using multiple isomorphous replacement (MIR) methods. Table 1 gives the details and statistics for the data collection and phasing procedure.

The crystal asymmetric unit contains three protomer complexes, each of which consists of an α and a β apoprotein, three Bchl *a* molecules, one carotenoid and a detergent molecule (β-octylglucoside). The electron density map allows a tracing of residues 1–47 of the α-apoprotein, all of the β-apoprotein and all the pigments. Twenty-two water molecules have been positioned. Figure 1 shows two regions of the initial electron density map.

The overall assembly

The structure of the active assembly may be described simply. The transmembrane helices of nine α-apoproteins are packed side by side to form a hollow cylinder of radius 18 Å. The nine helical β-apoproteins are arranged radially with the α-apoproteins to form an outer cylinder of radius 34 Å. The α-apoprotein helices are parallel to the ninefold axis to within 2°, and the β-apoprotein helices are inclined by 15° relative to this axis. The pigment molecules are contained between these inner and outer protein walls. The Bchl *a*-binding histidines of the α (His 31) and β (His 30) apoproteins face outwards and inwards, respectively, forming a complete ring of 18 overlapping Bchl *a* molecules. For these molecules, the planes of the bacteriochlorins are parallel to the membrane normal and their centres are approximately 10 Å from the presumed periplasmic membrane surface. The nine remaining Bchl *a* molecules are packed between the β-apoprotein helices a further 16.5 Å into the membrane with their bacteriochlorin rings parallel to the membrane surface. There is an elegant intertwining of the carotenoid molecules and the phytol chains of both sets of Bchl *a* molecules. Figure 2 shows the arrangement of the nonameric assembly. The current agreement of 0.25 Å between the α-carbons of the three crystallographically independent protomers suggests exact ninefold symmetry of the assembly.

§ To whom correspondence should be addressed.

TABLE 1 Crystallographic structure determination

Data set	No. crystals	Resolution (Å)	Completeness (%)	R_{merg} (%)	R_{iso} (%)	No. sites	Phasing power acentric (centric)	R_{cull}
Native(1)	1	3.00	99.0	3.0				
Native(2)	9	2.50	98.9	5.0				
K_2HgI_4	1	3.00	93.4	3.6	11.7	6	0.9 (0.8)	0.83
Pt combined	1	3.00	90.6	3.7	12.8	6	1.4 (1.0)	0.71
$K_2Pt(CN)_4$	1	3.00	96.8	3.3	13.0	3	1.0 (1.0)	0.67
K_2PtCl_4	1	3.00	95.8	3.8	11.1	3	1.5 (1.2)	0.57

Data collection. Derivative soaks were characterized with data collected using a Siemens area detector on a rotating-anode source and an image plate on the Daresbury synchrotron radiation source (SRS). A native data set, and derivative sets for the K_2HgI_4 and Pt combined soaks were collected at station 9.6 at the Daresbury Synchrotron. Additionally, derivatized crystals were back-soaked in artificial mother liquor for short periods and data sets collected. All data were collected at a wavelength of 0.87 Å, providing anomalous signals close to optimal magnitudes for the derivatives. **Derivative data and Patterson solution.** Diffraction data from the 30 cm MAR image plate at station 9.6 were processed with the program MOSFLM[14]. Despite a high degree of thermal diffuse scatter, data of high quality were collected from single crystals including a native data set to 3.0 Å resolution. Difference Pattersons derived from structure factors of soaked and back-soaked data sets clearly showed a subset of heavy atom sites. The coordinates of these sites were obtained from SHELX-S[15] in Patterson search mode. Cross-phasing using these subsets of sites with native and derivative amplitudes yielded all sites for the two derivatives. Subsequently the Pt combined soak was separated into the active reagents detailed above, and data sets were again collected under equivalent conditions at station 9.6. MIR sites were refined for the $K_2Pt(CN)_4$, K_2PtCl_4 and K_2HgI_4 derivatives to their isomorphous limit of 4.0 Å. **Phase improvement.** The MIR phases were extended to the derivative data limit and the phase set improved using solvent flattening and histogram matching[16,17] phase extension. Solvent flattening procedures were undertaken with the program DM[18]. The mask was derived using the Wang[19] method with a sphere of radius 10 Å and an estimated 55% solvent content (the estimate[20] from the calculated V_m is 73%). The resulting map showed all of the salient details of the complex and revealed a nonameric arrangement of protein subunits sharing a common rotation axis with the crystallographic three-fold. Non-crystallographic symmetry averaging was used to improve the map and extend the phase set to the limit of the native(2) data. The toroidal protein envelope of cylindrical radii 10 Å and 45 Å was subdivided into 40° segments and averaged with DM. The volume averaged comprised 3 × 13% of the unit cell. This resulted in an improved map with an R_{free} (ref. 21) of 23%, correlation coefficients in the range 0.95–0.96 between the three equivalent segments, and a mean figure of merit of 0.78 for the phase set. **Model building and refinement.** The map was of a very high quality with continuous density throughout. The crystallographic asymmetric unit of the complex was built with the program O[22] using a combination of the solvent-flattened MIR map and the non-crystallographic symmetry-averaged map. The alignment of the protein sequence was aided by the location of α Met 1, and the well-characterized Bchl *a*-contacting histidines at α 31 and β 30. A seleno–methionine modified complex had been crystallized, and anomalous difference amplitudes from these crystals, phased with the MIR phase set, indicated the Met sulphur site in the native complex. The initial model (R_{cryst} 43%) was refined using several refinement strategies with the XPLOR[23] and PROLSQ[24] programs. Individual atomic temperature factors were refined isotropically. The current model comprises a total of 3,345 non-hydrogen atoms in the crystallographic asymmetric unit. The current R_{cryst} and R_{free} (calculated with 4.6% of reflections) over the resolution interval 12.0–2.5 Å are 23.7 and 29.2%, respectively, for 27,855 independent reflections ($F > 2\sigma F$). The diffraction patterns display pronounced thermal diffuse scatter, suggesting anisotropic thermal motion which the isotropic refinement has not modelled. The r.m.s. deviations of the model from target geometries are 0.023 Å for bond lengths and 3.4° for bond angles. The atomic coordinates will be deposited in the Brookhaven Protein Data Bank when the refinement is completed. All computations used programs from the CCP4 Suite[18], except where explicitly stated. $R_{merg} = \Sigma_h \Sigma_j |I(h) - I(h)_j| / \Sigma_h \Sigma_j I(h)_j$, where $I(h)$ is the mean intensity for reflection **h**, after rejection of outliers. $R_{iso} = \Sigma_h ||F_{PH}| - |F_P|| / \Sigma_h |F_P|$, where $|F_{PH}|$ and $|F_P|$ are, respectively, the derivative and native structure factor amplitudes. Phasing power $= \Sigma_h |F_{H\,calc}| / \Sigma_h \varepsilon$, where $|F_{H\,calc}|$ is the calculated structure factor amplitude for the heavy atom, and ε is the residual lack of closure (of the vector triangle $|F_P|$, $|F_{PH}|$ and $|F_{H\,calc}|$) for reflection **h** (calculated for acentric and centric reflections over the resolution interval 16.0–4.0 Å). $R_{cull} = \Sigma_h ||F_{PH} - F_P| - |F_{H\,calc}|| / \Sigma_h ||F_{PH}| - |F_P||$, where $|F_{PH}|$, $|F_P|$ and $|F_{H\,calc}|$ are defined above (summed over centric reflections). Figure of merit $= \langle \cos(\Delta\alpha_h) \rangle$, where $\Delta\alpha_h$ is the error in phase angle for reflection **h**: a figure of merit of 0.78 corresponds to a phase error of 38.7°.

The arrangement of this assembly differs markedly from that in the plant light-harvesting complex[10], where the gross assembly is formed from a trimer of complexes. Each monomer is formed from a single polypeptide chain forming a pair of tilted helices surrounded by pigment molecules and an adjacent third helix which is almost parallel to the membrane normal. The seven Chl *a* and five Chl *b* molecules in that structure have the planes of the porphyrins tilted to the membrane normal and are arranged in six separate clusters. Two carotenoid molecules span the membrane, contacting each Chl *a* and binding the core of helices together like a crossbrace.

The apoprotein subunits

Each apoprotein subunit forms a single helix spanning the membrane bilayer with the amino (N) terminus on the cytoplasmic side[3]. In the α-apoprotein the N-terminal residue is buried approximately 9 Å from the presumed membrane surface, and coordinates to the central magnesium atom of a Bchl *a*. Although the published amino-acid sequence[3] has this N-terminal residue as methionine, the electron density is best fitted with a formylmethionine (fMet), where the Mg coordination is through the formyl oxygen (Fig. 1). The methionine sulphur atom is excluded as a possible ligand as its position has been accurately determined by a seleno–methionine derivative. The position of the sulphur atom restricts the possible movement of the terminal amine towards the Mg atom at the centre of the bacteriochlorin. A coordination, mediated by a water molecule, to the N terminus of a methionine residue was considered but rejected as it does not give a satisfactory fit to this density. Residues 2 to 9 form nearly 3 turns of a 3_{10}-like helix. This amphipathic helix lies on the presumed membrane surface with Ile 6, Trp 7 and Val 9 directed into the hydrophobic interior, and the side chains of Gln 3, Lys 5 and Thr 8 extending below the presumed surface. There is a turn at Asn 11–Pro 12, allowing residues 11 to 36 to form the membrane-spanning helix. Another turn at Thr 38 leads to a second amphipathic helix lying along the presumed periplasmic surface of the membrane. Like the N-terminal helix, this has hydrophobic residues (Trp 40, Phe 41, Tyr 44, Trp 45) directed into the membrane and hydrophilic residues (Thr 39, Gln 46) above the presumed surface. These N- and carboxy (C)-terminal helices appear to anchor the transmembrane helix nearly perpendicular to the membrane surfaces. The fold of the β-apoprotein is similar, although the shorter sequence is reflected in shorter N- and C-terminal locating structures. The first five residues of the β-apoprotein lie on the presumed membrane surface in an extended conformation with alternating hydrophobic residues (Ala 1, Leu 3, Ala 5) inserted into the membrane. Two turns of an irregular helix lead to the membrane-spanning α-helix from residue 11 to residue 36. A turn at Thr 37–Pro 38 leads to a short C-terminal tail where Pro 38, Trp 39 and Leu 40 anchor the helix to the presumed periplasmic membrane surface. Figure 3 shows the arrangement of the α- and β-apoproteins in the protomer.

Unexpectedly, the only direct interaction between the helices is at the N- and C-terminal ends. Within membrane-buried portions of the helices, interactions are mediated via the pigment

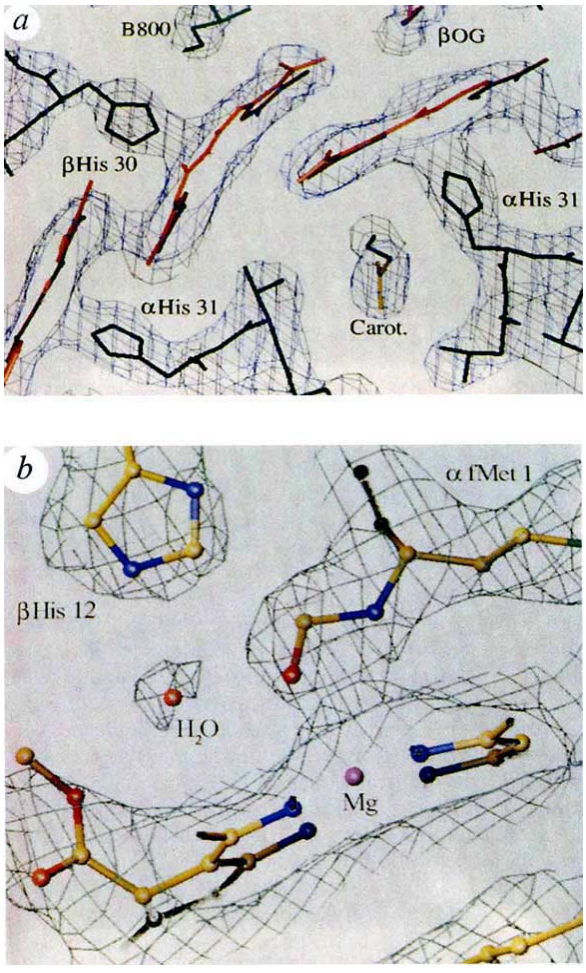

FIG. 1 Two regions of the electron density (MIR-phased, solvent-flattened, and averaged) used to determine the structure. *a*, The arrangement of apoproteins and B850 Bchl *a* molecules viewed down the crystallographic three-fold axis. Proteins are shown as black, B850 Bchl *a* red, carotenoids yellow, and the end of a B800 Bchl *a* phytol chain green. Adjacent to this a detergent molecule is coloured magenta. *b*, A B800 Bchl *a*, with the additional density at the N terminus of an α-apoprotein, is in the centre. A fitted formyl group and an adjacent buried water molecule are also shown. Atoms are colour-coded red for oxygen, blue for nitrogen, yellow for carbon, magenta for magnesium and green for sulphur.

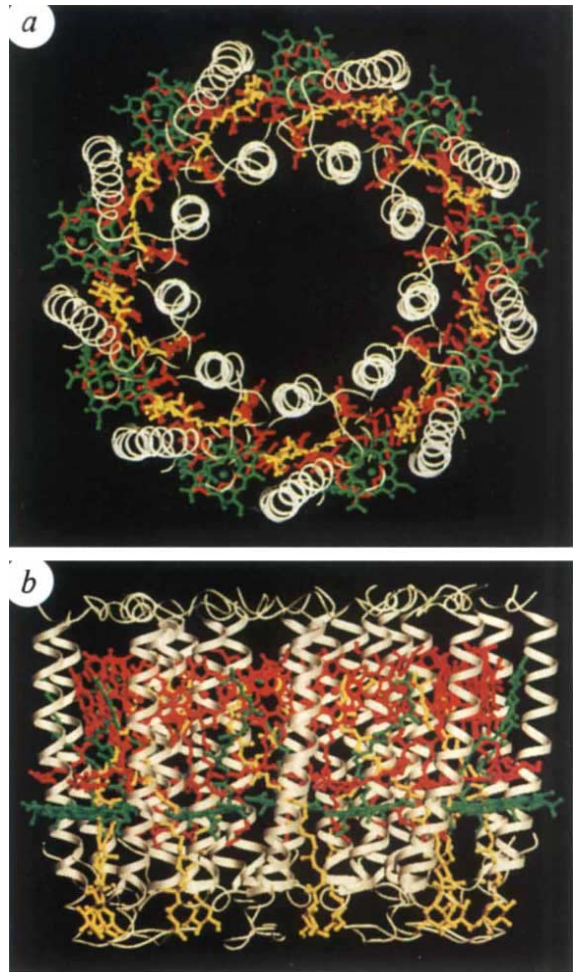

FIG. 2 *a*, The nonameric complex viewed from the cytoplasmic side of the membrane. Protein units are shown as white, B800 Bchl *a* green, B850 Bch *a* red, and carotenoid yellow. *b*, The complex viewed perpendicular to the symmetry axis. Broad ribbons, beginning at the level of the amphipathic helix axis on the periplasmic side and at the level of a buried water molecule (not shown) on the cytoplasmic side, indicate the presumed hydrophobic region of the membrane.

molecules or buried water. This lack of helix–helix interaction, and the predominance of pigment–protein interactions, probably explains why all models[11] of the structure of this complex, which assumed helix–helix contacts, were wrong. At the N terminus, the association of the postulated α fMet 1 with a buried Bchl *a* restricts the protein–protein interactions to the radially associated α- and β-apoproteins. At the C terminus there are interactions between radial and adjacent α- and β-apoproteins and between adjacent α-apoproteins. In particular, the large aromatic residues (α Trp 40, Trp 45, Tyr 44, and β Trp 39) are involved in binding the apoproteins together through hydrogen bonds and hydrophobic interactions.

Apart from β Arg 20 and Asp 17, which form an ion pair on the outer face, both transmembrane surfaces of the nonamer are hydrophobic. No ordered molecules have yet been identified in the hydrophobic central channel of the complex.

Bacteriochlorophyll *a*

The Bchl *a* molecules form two groups. One group of nine well-separated molecules is located between the β-apoprotein helices, and another group of eighteen forms a closely interacting ring. Based on previous spectroscopic studies on this and several homologous LH2 complexes[1–3,5,6], the group of nine can be identified as the Bchl *a* molecules that absorb at 800 nm (B800 Bchl *a*) and the ring of eighteen as those that absorb at 850 nm (B850).

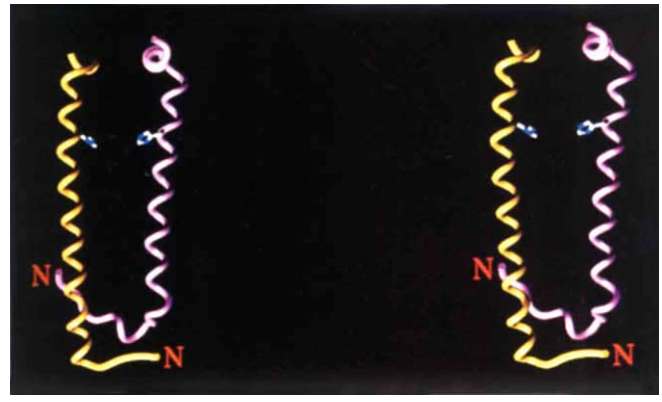

FIG. 3 A stereo view of the α (magenta) and β (yellow) apoproteins in the crystallographic protomer shown as a ribbon trace. The position of the His residues which ligand the B850 Bchl *a* molecules are shown.

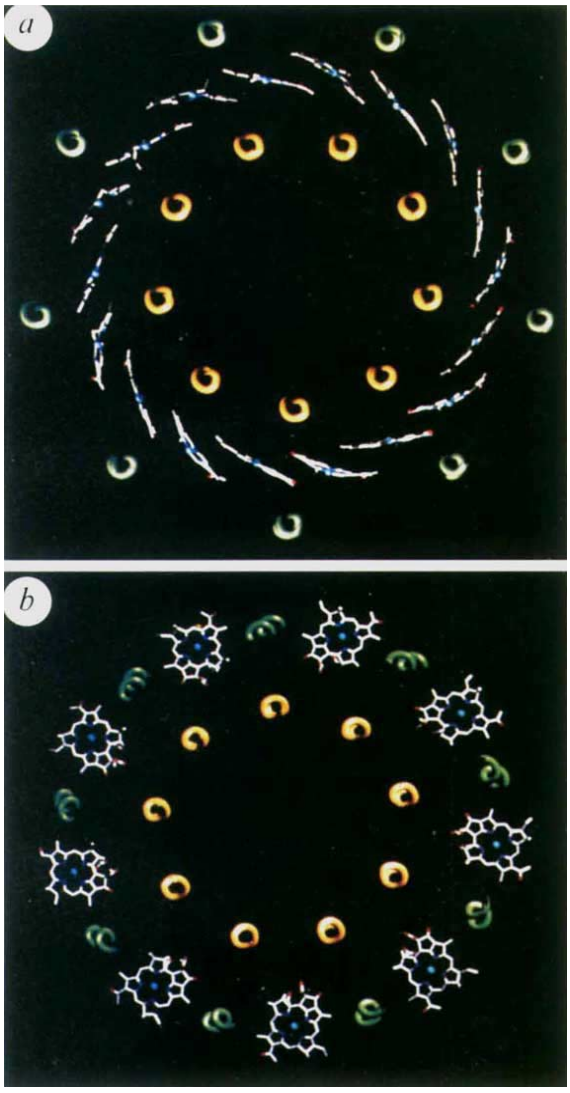

FIG. 4 *a*, The ring of B850 Bchl *a* molecules. *b*, The positions of the B800 Bchl *a* molecules between the helices of the *β*-apoproteins forming the outer cylindrical wall of the complex. The α-apoproteins are coloured yellow and the β-apoproteins green.

The eighteen B850 Bchl *a* molecules are supported by histidine residues on the α- and β-apoproteins with their bacteriochlorin rings perpendicular to the membrane surface and associated phytol chains descending into the hydrophobic core of the assembly. In contrast, the B800 Bchl *a* molecules have their bacteriochlorin rings aligned parallel to the membrane surface, are linked to a proposed formyl oxygen of an amino-terminal fMet of the α-subunit, and have their phytol chains directed up into the middle of the complex assembly.

Although the B850 nm Bchl *a* molecules form a complete overlapping ring (Fig. 4*a*), their molecular environments are not all equivalent. Within a protomer, the Mg–Mg distance is 8.7 Å, and between adjacent protomers, it is 9.7 Å. There are van der Waals contacts at the periphery of the bacteriochlorin systems. The conformations of the phytol chains of the α and β B850 Bchl *a* molecules differ (Fig. 5). In the α form the chain is slightly more extended, whereas in the β form the chain is bent to allow it to curve around the phytol chain rising from the B800 Bchl *a* coordinated to an adjacent α-apoprotein.

The nine B800 Bchl *a* molecules are located between β-apoproteins, with the planes of the bacteriochlorins parallel to the presumed cytoplasmic membrane surface and at a distance of about 11 Å from it (Fig. 4*b*). The distance between the central Mg atoms of these Bchl *a* molecules is 21 Å. The pigment is held in this position by coordination of the central Mg to the carbonyl oxygen of the putative N-terminal fMet as discussed above. Coordination from the N terminus to the central metal of a porphyrin/bacteriochlorin system is unusual and has been observed in only one other structure[12]. The phytol chain projects up into the interior of the complex where it contacts the B850 Bchl *a* coordinated to the same apoprotein. The conformation of the chain differs again from that in the α and β B850 Bchl *a* molecules. Although the B850 molecules interact by overlapping at the edges of the bacteriochlorin systems, the closest interaction between B800 and B850 molecules is through the intertwined phytol chains. The phytol chain from the β B850 bacteriochlorophyll bends and passes parallel to the B800 bacteriochlorin ring at a distance of 4.0 Å, close enough for van der Waals contact. The distance between the central Mg atoms of the closest pair of B800 and B850 molecules is 17.6 Å.

There is a distinct difference in the environment of the two sets of Bchl *a* molecules. The pigments that absorb at 850 nm are in a hydrophobic environment, with α Ala 27, Ile 34, Trp 45 and β Phe 22, Ala 26, Trp 39 making a number of contacts. The only hydrogen bonds formed are from α-apoproteins: to the bacteriochlorin ring-B acetyl carbonyl oxygen from NE1 of Trp 45 for α-coordinated Bchl *a* molecules, and from OH of Tyr 44 (on an adjacent α-apoprotein) for β-coordinated ones. In contrast, the molecules that absorb at 800 nm are in a relatively polar environment, with water located between β His 12, the ring-D ester carbonyl oxygen, and the putative formyl group coordinated to the central Mg (Fig. 1). A strong hydrogen bond is formed from the Arg 20 side chain of a β-apoprotein to the ring-B acetyl carbonyl oxygen. There are few van der Waals contacts with hydrophobic protein residues.

Carotenoid

In the B800–850 LH2 complex of *Rps acidophila*, the carotenoid, rhodopin-glucoside, absorbs visible light. Estimates of the stoichiometric amount of carotenoid in the complex suggested a carotenoid:Bchl ratio of 1:2 (refs 2, 4) that is, there are 13–14 molecules for this assembly. The crystal structure shows one carotenoid molecule for each protomer of α- and β-apoproteins. It is uncertain whether the observed detergent molecule has replaced a second carotenoid in the protomer. The observed carotenoid is not associated with any single apoprotein. It has an extended conformation and spans the depth of the membrane, beginning with its glucosyl ring associated with Lys 5 and Thr 8 of an α-subunit. On its path through the complex, it makes

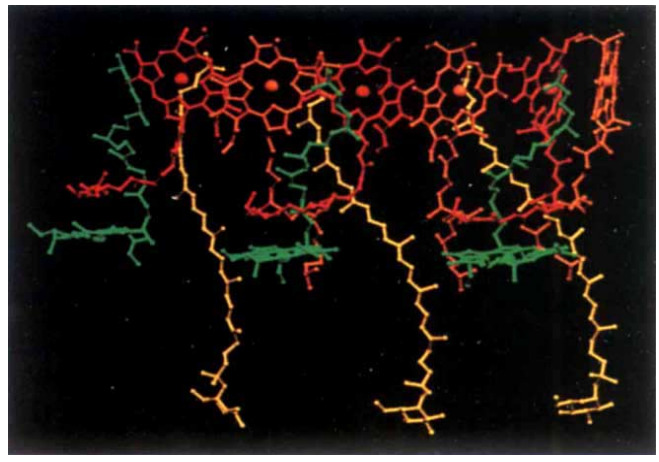

FIG. 5 The arrangement of the pigments in the asymmetric unit. B800 Bchl *a*, green; B850 Bchl *a* bound to α-apoproteins, orange; those bound to β-apoproteins, red; and carotenoid, yellow.

several van der Waals contacts (<3.5 Å) with hydrophobic residues of adjacent β and α apoproteins and with both B850 and B800 Bchl *a* molecules. It finishes with its terminal dimethyl groups in contact with His 31 of the adjacent α-apoprotein. It is this residue that is bound to the central Mg of a B850 Bchl *a*. The arrangement of the pigments in the asymmetric unit is shown in Fig. 5.

Energy transfer mechanism

When a Bchl molecule is excited by light, its first excited singlet state lasts for a few nanoseconds[1]. The light-harvesting system must be able to transfer the absorbed energy to the reaction centre in a shorter time than this. Some of the important features that allow this to take place are revealed by the structure reported here.

Previous biophysical studies (reviewed in ref. 1) have shown that energy transfer within the LH2 complex can occur from the B800 to the B850 BChl *a* molecules in 0.7 ps. Once the energy reaches the B850 molecules, it is rapidly transferred among them. This is seen as an ultrafast depolarization of the excited state on the 200–300 fs timescale. Energy transfer from LH2 to LH1 occurs in the 5–20 ps time range, but with LH2 alone the decay of the 850 nm excited singlet state takes 1.1 ns.

The ring of B850 Bchl *a* molecules acts rather like a 'storage ring', with the excited state rapidly delocalized over a large area. The delocalization is facilitated by a highly hydrophobic environment which reduces the dielectric constant, allowing coupling over large distances. The energy is then available for transfer from any part of the ring to any neighbouring LH1 complex. It is clear from electron microscopy imaging of the LH1 complex[13], and from a comparison of the primary structures[3] of the LH2 and LH1 complexes, that the structure of the LH1 complex is similar to that of LH2 (with a larger ring). With such a ring structure, there is no requirement for the LH1 complex to have a special orientation to receive energy from the LH2 ring. Furthermore, because the B875 Bchl *a* molecules in LH1 are liganded to homologous histidine residues, as in LH2, it is likely that the B850 and B875 bacteriochlorophyll rings will be at the same point in the membrane. The overall effect will be to allow energy transfer from any LH2 to any LH1 complex that is within range, without regard to the orientation of either complex. This reduction in the dimensionality of the process will lead to a further kinetic gain.

Previous studies have shown that the carotenoid in this LH2 complex acts as an efficient accessory light-harvesting pigment (>50%)[7]. The excited singlet lifetime of carotenoids is usually less than 10 ps[8]. Therefore, if energy transfer is to compete successfully with these rapid de-excitation processes, the carotenoid must be located very close to the acceptor bacteriochlorophylls[8], as seen in the structure. □

Received 29 December 1994; accepted 13 February 1995.

1. van Grondelle, R., Dekker, J. P., Gillbro, T. & Sundstrom, V. *Biochim. biophys. Acta* **1187,** 1–65 (1994).
2. Hawthornthwaite, A. M. & Cogdell, R. J. in *The Chlorophylls* (ed. Scheer, H.) 493–528 (CRC, Boca Raton, 1993).
3. Zuber, H. & Brunisholz, R. A. in *The Chlorophylls* (ed. Scheer, H.) 627–704 (CRC, Boca Raton, 1993).
4. Gardiner, A. T., Cogdell, R. J. & Takaichi, S. *Photosyn. Res.* **38,** 159–168 (1993).
5. Cogdell, R. J. & Scheer, H. *Photochem. Photobiol.* **42,** 669–689 (1985).
6. Robert, B. & Lutz, M. *Biochim. biophys. Acta* **807,** 10–23 (1985).
7. Angerhofer, A., Cogdell, R. J. & Hipkins, M. F. *Biochim. biophys. Acta* **848,** 333–341 (1986).
8. Frank, H. A. & Cogdell, R. J. in *Carotenoids in Photosynthesis* (eds Young, A. & Britton, G.) 252–326 (Chapman & Hall, London, 1993).
9. Papiz, M. Z. *et al. J. molec. Biol.* **209,** 833–835 (1989).
10. Kuhlbrandt, W., Wang, D. N. & Fujiyoshi, Y. *Nature* **367,** 614–621 (1994).
11. Olsen, J. D. & Hunter, C. N. *Photochem. Photobiol.* **60,** 521–535 (1994).
12. Martinez, S. E., Huang, D., Szczepaniak, A., Cramer, W. A. & Smith, J. L. *Structure* **2,** 95–105 (1994).
13. Karrasch, S., Bullough, P. A. & Ghosh, R. *EMBO. J.* **14,** 631–638 (1995).
14. Leslie, A. G. W. in *Joint CCP4 and ESF-EACMB Newsletter on Protein Crystallography* No. 26 (Daresbury Laboratory, Warrington, 1992).
15. Sheldrick, G. M. *Acta crystallogr.* A**46,** 467–473 (1990).
16. Zhang, K. Y. J. & Main, P. *Acta crystallogr.* A**46,** 377–381 (1990).
17. Cowtan, K. D. & Main, P. *Acta crystallogr.* D**49,** 148–157 (1993).
18. Collaborative Computational Project, No. 4 *Acta crystallogr.* D**50,** 760–766 (1994).
19. Wang, B. C. *Meth. Enzym.* **115,** 90–112 (1985).
20. Matthews, B. W. *J. molec. Biol.* **33,** 491–497 (1968).
21. Brunger, A. T. *Nature* **335,** 472–475 (1992).
22. Jones, T. A., Zou, J. Y., Cowan, S. W. & Kjeldgaard, M. *Acta crystallogr.* A**47,** 110–119 (1991).
23. Brunger, A. T. *XPLOR Version* 3.1 *Manual* (Yale Univ., USA, 1993).
24. Hendrickson, W. A. *Meth. Enzym.* **115,** 252–270 (1985).

ACKNOWLEDGEMENTS. We thank P. Emsley for help with general computations. Some diffraction data were collected at the EMBL synchrotron source, Hamburg, and the assistance of K. S. Wilson and Z. Dauter is gratefully acknowledged. This work has been supported by the BBSRC Membrane Initiative and the E.C. R.J.C. dedicates this paper to H. Zuber and J. P. Thornber, fathers of this area of research.

Observational confirmation of a circumsolar dust ring by the COBE satellite

W. T. Reach*, B. A. Franz†, J. L. Weiland‡, M. G. Hauser§, T. N. Kelsall§, E. L. Wright‖, G. Rawley†, S. W. Stemwedel† & W. J. Spiesman¶

* Universities Space Research Association, NASA Goddard Space Flight Center, Code 685, Greenbelt, Maryland 20771, USA
† Applied Research Corporation, ‡ General Sciences Corporation, NASA GSFC, Code 685.3, Greenbelt, Maryland 20771, USA
§ NASA GSFC, Code 680, Greenbelt, Maryland 20771, USA
‖ UCLA Astronomy Department, Los Angeles, California 90024, USA
¶ McDonald Observatory, University of Texas, Austin, Texas 78712, USA

ASTEROID collisions are an important source of the dust particles in the zodiacal cloud[1–3]. These particles spiral in towards the Sun under the influence of drag forces[4–6] and, in passing through the inner Solar System, are subject to gravitational perturbations by the planets, which may trap them (at least temporarily) in orbital resonances[7–10]. Recently, numerical simulations have shown that resonances with the Earth are particularly effective at trapping asteroidal dust, leading to the suggestion that the Earth may be embedded in a circumsolar ring of dust[11]. The azimuthal structure of this ring was predicted to be asymmetric, with the region trailing the Earth being substantially more dense than that in the leading direction[11]. This prediction is in both qualitative and quantitative agreement with the asymmetry in zodiacal light observed by the Infrared Astronomical Satellite (IRAS)[11,12], but the IRAS data alone are equivocal because of calibration uncertainties and sparse coverage of elongation angle[12]. Here we report observations by the Diffuse Infrared Background Experiment[13] (DIRBE) on the Cosmic Background Explorer satellite (COBE)[14], which confirm both the existence of this ring and the predictions of its near-Earth structure.

DIRBE mapped the entire sky with a 0.7° beam in ten wavebands (1.25, 2.2, 3.5, 4.9, 12, 25, 60, 100, 140 and 240 μm). The DIRBE instrument measured the sky brightness relative to an internal zero-brightness reference source, thus eliminating the calibration uncertainty of IRAS. The viewing geometry for DIRBE is illustrated in Fig. 1. The COBE satellite orbits the Earth along the terminator, and it spins at 0.8 r.p.m. about an axis nearly perpendicular to the Earth–Sun line. The DIRBE field of view is offset 30° from the spin axis. The combination